Improved structural model of Pb-doped γ-Bi_2O_3: $(Bi_{23.68}Pb_{0.32})(Bi_{1.28}Pb_{0.72})O_{38.48}$

Aleksandra Dapčević,[1,a)] Dejan Poleti,[1] and Ljiljana Karanović[2]
[1]*Faculty of Technology and Metallurgy, University of Belgrade, Karnegijeva 4, 11000 Belgrade, Serbia*
[2]*Faculty of Mining and Geology, University of Belgrade, Đušina 7, 11000 Belgrade, Serbia*

(Received 26 December 2011; accepted 29 December 2011)

A polycrystalline single-phase sample with nominal composition $Bi_{24}PbO_{37}$ was synthesized from Bi_2O_3 and PbO by a high-temperature solid state reaction at 690 °C for 1.5 h. The compound adopts $Bi_{12}SiO_{20}$-type structure [cubic, space group *I*23 (No. 197); $a = 10.24957(3)$ Å] and was refined to $R_p = 7.96\%$, $R_{wp} = 10.4\%$, $R_{exp} = 8.43\%$, $R_B = 3.06\%$, and $S = 1.23$. The distributions of Pb^{2+} and Bi^{3+} over cationic sites based on the X-ray powder diffraction data were determined using a combination of the Rietveld refinement and bond valence calculations. The results showed that the asymmetric unit contains two mixed cation sites: the fully occupied 24*f* site and the partly occupied 8*c* site, with the unit-cell content $(Bi_{23.68}Pb_{0.32})(Bi_{1.28}Pb_{0.72})O_{38.48}$. The structural constraints favor a preference of Pb^{2+} ion for the 8*c* site, i.e. only 1.3% of Bi^{3+} is substituted by Pb^{2+} at the 24*f* site and 36% at the 8*c* site. At the 24*f* site, the cations are surrounded by $5 + 2$ or in a very small amount by $5 + 1 + 2$ oxide ions, forming a base bicapped square pyramid or a bicapped highly deformed octahedron, respectively. At the 8*c* site, the cations with three oxide ions form a trigonal pyramid with the cations at the apex. © *2012 International Centre for Diffraction Data.*
[doi:10.1017/S0885715612000073]

Key words: $Bi_{24}PbO_{37}$, sillenite, crystal structure, Rietveld refinement, bond valence, mixed sites

I. INTRODUCTION

Bismith(III) oxide exhibits an extraordinary rich phase polymorphism appearing in seven modifications: monoclinic α-, tetragonal β-, body-centered cubic γ-, face-centered cubic δ-, orthorhombic ε-, triclinic ω-, and a high-pressure hexagonal phase (Sillén, 1937; Gattow and Schröder, 1962; Levin and Roth, 1964a; Harwig, 1978; Harwig and Weenk, 1978; Harwig and Gerards, 1979; Gualtieri *et al.*, 1997; Sammes *et al.*, 1999; Cornei *et al.*, 2006; Ghedia, *et al.*, 2010). Among these seven polymorphisms, metastable γ- and high-temperature δ-Bi_2O_3 are found to be the most investigated because of their interesting structural and other properties. The high-temperature δ-Bi_2O_3 modification can be stabilized at room temperature by using many isovalent and aliovalent cations to substitute Bi^{3+} (Shuk *et al.*, 1996; Sammes *et al.*, 1999), but this often causes the formation of modulated structures based on a fluorite-related substructure (Watanabe, 1997; Pang *et al.*, 1998; Darriet *et al.*, 2005). The metastable γ-Bi_2O_3 phase can also be stabilized down to room temperature by doping with many different cations, and in that case the structural features depend on the size, oxidation state, and concentration of dopant (Levin and Roth, 1964b).

The title compound is one of the doped γ-Bi_2O_3 phases belonging to the $Bi_{12}SiO_{20}$ (sillenite) structure type. There are two cation sites in this structure: general 24*f* and special 2*a*. The cation, labeled as Bi1, is positioned at the 24*f* site, while the dopant cation, *M*, is positioned at the 2*a* site, i.e. in the origin and center of the *bcc* unit cell (space group *I*23). As long as the charge of dopant is 4+, the crystal structure is composed of $Bi1O_7$ polyhedra and ideal MO_4 tetrahedra. Five oxygen atoms at shorter distances form a distorted square pyramid, and with two other oxygen atoms at very long distances create a $5 + 2$ coordination polyhedron around Bi1. According to bond valence (BV) calculations (Poleti *et al.*, 2007), the contribution of two distant oxygen atoms to the bond valence sum of $Bi1^{3+}$ ion is negligible (usually <3%), i.e. the coordination number of Bi1 can be described as five. Two square pyramids share a common edge and two pairs of adjacent pyramids are connected by the MO_4 tetrahedra along [100]. Thus, two pairs of pyramids with two MO_4 tetrahedra form a cavity that contains the $6s^2$ lone electron pairs of Bi^{3+} ions.

If the charge of the *M* cation is less than 4+, the stoichiometry is more complicated, and the formulae of corresponding doped sillenite phases can be calculated from the general formula $Bi1_{12}(Bi2^{3+}_{(4-n)/(5-n)}M^{n+}_{1/(5-n)})O_{19+1/(5-n)}$ assuming full occupancy of both cationic sites (Valant and Suvorov, 2002). For such phases, two basic structural models have been proposed by Craig and Stephenson (CS-model; Craig and Stephenson, 1975) and by Radaev (R-model; Radaev *et al.*, 1991; Radaev and Simonov, 1992). According to the CS-model, $Bi2^{5+}$ and M^{n+} ions share the 2*a* site. Previously, by analysis of the geometry parameters and results of BV calculations for 30 structurally characterized sillenites, it was shown that the R-model is more acceptable (Poleti *et al.*, 2007). This means that *M* cations and $Bi2^{3+}$ ions are slightly moved from the origin along the [111]-direction to the 8*c* site. Also, the vacancies of O atoms should be introduced for charge balance. The deficiency of positive charge is compensated for by a partial occupancy of O3 atoms forming a trigonal pyramid instead of tetrahedral coordination of the 8*c* site. If the dopant is a Pb^{2+} ion, the formula of the corresponding γ-Bi_2O_3 phase is $Bi_{12}(Bi_{2/3}Pb_{1/3})O_{19.33}$ or $Bi_{38}PbO_{58}$.

[a)] Author to whom correspondence should be addressed. Electronic mail: hadzi-tonic@tmf.bg.ac.rs

0885-7156/2012/27(1)/2/6/$18.00

If the charge of the *M* cation is 5+, then the occupancy of the 2*a* site should be limited to 0.80. However, there is at least one sillenite, $Bi_{12.03}V_{0.89}O_{20.27}$, where the occupancy of the 2*a* site exceeds 0.80 (Radaev and Simonov, 1992). In this case, an excess of positive charge is compensated for by a partial occupancy of the 6*b* site (the middle of the unit-cell edges) with an additional O4 atom.

As was shown in our previous work on sillenites (Poleti *et al.*, 2007), considering the geometry parameters and oxidation numbers of *M* cations, new structural characterizations are needed for at least three systems: Co-, Mn-, and Pb-doped γ-Bi_2O_3. To explore their structural complexity, we began to investigate Pb^{2+}-incorporating sillenites. Our earlier (Poleti *et al.*, 2007) and some new results (to be published) have revealed that single-phase Pb-doped γ-Bi_2O_3 specimens with Bi:Pb ratios of 11:1, 12:1, 24:1, 36:1, and 38:1 can easily be prepared by high-temperature solid state reaction. Also, the application of some other treatments, such as mechanochemical synthesis, allows the preparation of Pb-doped γ-Bi_2O_3 even from starting mixtures with 1:1 and 2:1 Bi:Pb ratios (Zyryanov, 2004). Independently of the type of synthesis, the Pb-doped γ-Bi_2O_3 unit-cell parameters are very close to those of undoped γ-Bi_2O_3, which is a logical consequence of the great similarity of Bi^{3+} and Pb^{2+} ions: they are isoelectronic, with similar ionic radii, and both have the lone electron pair.

Previously, Murray *et al.* (1986) described the structure of $Bi_{12}PbO_{19}$. The analysis was performed using high-resolution neutron powder diffraction data. Two structural models, both of the CS type with some oxygen vacancies, were presented: the first with Pb^{2+} at the 2*a* site and Bi^{3+} at the 24*f* site, and the second with a random distribution of cations over the 2*a* and 24*f* sites. None of the models can be regarded as satisfactory, since the isotropic atomic displacement parameters (ADPs) of the cations at the 2*a* site were very high ($B_{iso} = 4.2$–5.3 Å^2) and the observed Pb–O distances were too short (1.95 Å). Besides, there are two papers describing the crystal structures of $Bi_{24}Pb_2O_{40}$ (Rangavittal *et al.*, 1994) and $Bi_{12}Pb_{0.89}O_{19.78}$ (Mazumdar, 1993) refined using X-ray powder diffraction data. In both cases, the presence of Pb^{4+} ions was assumed. However, these results are of very low reliability and will not be considered further. For example, the published unit-cell parameters are 10.292(8) Å for $Bi_{24}Pb_2O_{40}$ and 10.21 Å for $Bi_{12}Pb_{0.89}O_{19.78}$. Both values are well out of the range of known unit-cell parameters for Pb-doped γ-Bi_2O_3 phases, which are grouped at about 10.26 Å (Poleti *et al.*, 2007).

In addition to the very interesting structural properties, Pb-doped Bi_2O_3 phases also have a great potential application. For example, the mixed oxides from the Bi_2O_3–PbO system are good high-temperature ionic conductors, but also exhibit mixed ionic/electronic conductivity that could be useful in oxygen selective membranes (Honnart *et al.*, 1983; Fee and Long, 1996; Fee *et al.*, 1997). Next, mixed heavy metal oxide glasses based on Bi_2O_3 and PbO have interesting physical properties such as high density, high linear or non-linear refractive index, and long infrared cut-off (Pan and Ghosh, 2000; Knoblochova *et al.*, 2009; Reshak *et al.*, 2010; Shi and Qian, 2010; Salem and Mohamed, 2011). Moreover, the mixed Bi–Pb oxides with sillenite-type structure possess other extraordinary characteristics: they are wide-band-gap high-resistivity semi-insulating, photoconductive, photoluminescent, electronic, optoelectronic, acoustic, and piezoelectric materials (Mitsuyu *et al.*, 1976; Manier *et al.*, 1988; Sammes *et al.*, 1995; Borowiec *et al.*, 1999; Valant and Suvorov, 2001, 2002).

In this paper, we report the synthesis and detailed structural properties of Pb-doped γ-Bi_2O_3 with a Bi:Pb ratio of 24:1 investigated by X-ray powder diffraction, Rietveld analysis and BV calculations.

II. EXPERIMENTAL

A. Synthesis conditions

The yellow-orange polycrystalline sample with nominal composition $Bi_{24}PbO_{37}$ ($12Bi_2O_3 \cdot PbO$) was prepared by high-temperature solid state reaction. Stoichiometric amounts of bismite, α-Bi_2O_3 (99.975%, Alfa Aesar), and massicot, PbO (99.9%, Alfa Aesar), were dry homogenized for about 30 min in an agate mortar, heated at 690 °C for 1.5 h (heating rate 4 °C min^{-1}) in an open Pt crucible, and then annealed to room temperature.

B. Rietveld refinement

X-ray powder diffraction data of the re-ground polycrystalline product were collected using a SEIFERT XRD3000TT X-ray powder diffractometer with monochromated Cu*Kα* radiation ($\lambda = 1.5418$ Å) in a range 4–140° 2θ with a step-width of 0.02° and a constant counting time of 10 s per step. The FULLPROF software was used for the Rietveld refinement (Rodriguez-Carvajal, 1993) in WINPLOTR environment (Roisnel and Rodriguez-Carvajal, 2001).

The Rietveld refinement was performed adhering to the previously published recommendations (Karanović *et al.*, 1999; McCusker *et al.*, 1999). The profiles were described by the pseudo-Voigt function as the most frequently used function in this type of analysis (Young and Wiles, 1982; Hill, 1992; Hill and Cranswick, 1994), with n in $n \times$ FWHM equal to 30 and the limit for the peak asymmetry set to 90° 2θ. In the first stage of the refinement, the background was modeled using a linear interpolation between 80 selected points and in the last cycles of refinement the Fourier filtering method with the window size set to 2000 was used.

After an initial full-profile fitting, the structural refinement was performed by testing five structural models described later in detail. During the refinement of isotropic ADPs of O2 and O3 atoms, either non-positive ADP values were observed or the refinement became unstable. This can be explained by the significant difference between the X-ray scattering powers of Bi/Pb and O atoms. To avoid this problem, ADPs for all O atoms were restrained to be equal, i.e. O atoms were refined with a common isotropic ADP. This approach resulted in a rather acceptable common ADP value [1.7(3) Å^2]. In the final cycles of the refinement, a total of 21 parameters were refined using 6501 data points and 210 reflections. The site occupation factors were not refined.

C. Bond valence calculations

The bond valence calculations were performed using the equation $\sum v_{ij} = \sum \exp[(R_0 - R_{ij})/B]$ (Brown, 2009), where v_{ij}

is the bond valence for an interatomic bond, $\sum v_{ij}$ is the overall bond valence summed over all interatomic bonds of one ion, R_0 is the bond valence parameter that represents the length of a bond of unit valence and was taken to be 2.094 and 2.112 Å for Bi^{3+}–O and Pb^{2+}–O, respectively (Brese and O'Keeffe, 1991), R_{ij} is the experimentally obtained bond length and B is a 'universal' constant equal to 0.37 Å (Brown and Altermatt, 1985).

III. RESULTS AND DISCUSSION

A. Rietveld refinement and valence bond calculations

As mentioned in the Introduction, the formula $Bi_{38}PbO_{58}$ should represent the stoichiometrically ideal Bi:Pb molar ratio according to the R-model (Radaev *et al.*, 1991; Radaev and Simonov, 1992). However, we found that a single Pb-doped γ-Bi_2O_3 phase with the composition $Bi_xPbO_{3x/2+1}$ can be obtained in the relatively wide x range, $11 \leq x \leq 38$, indicating the possibility of isomorphous replacement of Pb^{2+} for Bi^{3+} at both crystallographic sites. The sample with composition $Bi_{24}PbO_{37}$ was chosen for this study because it was in the middle of the above interval.

At the beginning, the structural model published by Murray *et al.* (1986) with Pb^{2+} and Bi^{3+} at the 2*a* site was tested for comparison. Irrespective of whether the coordination around the 2*a* site is tetrahedral or trigonal, very similar results, i.e. very high ADPs for cations at the 2*a* site and O3 atom (about 4.0 and 3.0 Å^2, respectively), were obtained. These results clearly confirmed that CS-model (Craig and Stephenson, 1975) is inappropriate for the investigated sample.

Therefore, the R-model should be applied, which means that 2*a* cations are slightly displaced along the [111]-direction to the 8*c* site (with an occupancy of 0.25). This also caused an oxygen vacancy generation at the O3 position, resulting in the formation of a trigonal pyramidal geometry with a cation at the apex. Such coordination is asymmetrical and more favorable than a tetrahedral one for large Pb^{2+} and Bi^{3+} ions with their inert electron pairs. Actually, the presence of O3 vacancies was first suggested by Murray *et al.* (1986), but in their model Bi2 or Bi2/Pb2 cations were kept at the 2*a* site.

The main objective of this study was whether Pb^{2+} was preferentially situated at the 24*f* or 8*c* site. To test this, five structural models with the possible cation distributions were generated and refined by the Rietveld method. In all cases, it was assumed that no extra vacancies are present at both cationic sites, and a small amount of an additional O4 atom was placed at the 6*b* site to achieve charge balance.

The considered cation distributions over two sites indicated by formulae representing the unit-cell content are listed in Table I. In model A all Pb was placed at the 8*c* site, and in model E all Pb was placed at the 24*f* site. Model C was in accordance with the R-model and the content of the 8*c* site was $Bi_{1.33}Pb_{0.67}$, i.e. characteristic for M^{n+} cations with $n = 2$ (Valant and Suvorov, 2002). The cation distributions for models B and D were chosen to be exactly at the midpoints between A and C, and C and E, respectively. Therefore, the general formula for all structural models can be represented as $(Bi1^{3+}{}_{24-y}Pb1^{2+}{}_{y})(Bi2^{3+}{}_{2-x}Pb2^{2+}{}_{x})O_{38.48}$, where $x + y = 1.04$.

All parameters were refined as described in the Experimental section, but the results will not be described in detail because the refined coordinates of corresponding atoms, as well as most of their ADPs, were practically identical. For example, the common ADPs for cations distributed over the 8*c* site were 2.5(8) for model A, 2.6(8) for models B, C, and D, and 2.7(9) Å^2 for model E. Also, R_{wp} factors were equal for all five models (10.40%), whereas R_B factors were found to be in a very narrow range (3.05–3.07%). Apparently, these results were not useful to determine the most probable structural model. Since Pb^{2+} and Bi^{3+} as isoelectronic ions have a negligible difference in scattering power, the resolution between them is not possible by X-ray diffraction.

TABLE I. Cation distribution over two sites and comparison of BVS and OS values for the 8*c* site.

Model	Structural formula $(Bi1_{24-y}Pb1_y)(Bi2_{2-x}Pb2_x)$ $O_{38.48}$	Pb^{2+} content at 8*c* site (mole %)	BVS[a] (v.u.)	OS
A	$(Bi_{24})(Bi_{0.96}Pb_{1.04})O_{38.48}$	52	2.646	2.48
B	$(Bi_{23.80}Pb_{0.20})(Bi_{1.16}Pb_{0.84})O_{38.48}$	42	2.633	2.58
C	$(Bi_{23.63}Pb_{0.37})(Bi_{1.33}Pb_{0.67})O_{38.48}$	33	2.622	2.67
D	$(Bi_{23.29}Pb_{0.71})(Bi_{1.67}Pb_{0.33})O_{38.48}$	16	2.600	2.84
E	$(Bi_{22.96}Pb_{1.04})(Bi_{2.00})O_{38.48}$	0	2.580	3.00

[a] R_{ij} in equation $\sum v_{ij} = \sum \exp[(R_0 - R_{ij})/B]$ was 2.15 Å for all models.

To estimate cation distribution, bond valence analysis was performed and the results were compared with the calculated oxidation state (OS) of cations positioned at the 8*c* site (Table I). OS was calculated as a mean value considering the proposed Bi/Pb ratio and the charge of cations, i.e. 3+ and 2+, respectively. The BV sum (BVS) was calculated assuming that the 8*c* site is occupied by Bi or by Pb, and then averaged according to the Bi/Pb ratio. In an ideal case, BVS should be equal to OS, i.e. the BVS/OS ratio must be 1, and therefore model C seems to be very close to the most probable structural model (Table I).

The substitution of Pb^{2+} for Bi^{3+} at the 8*c* site causes an approximately linear increase of the BVS/OS ratio (Figure 1). The linear fit using the least-squares method

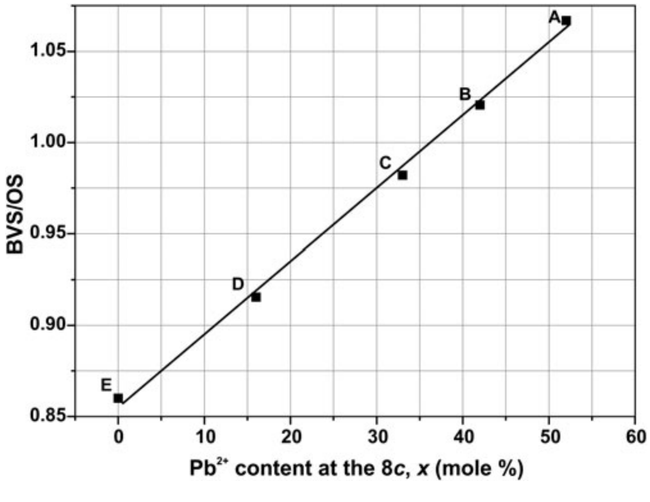

Figure 1. BVS/OS ratio vs. Pb^{2+} content at the 8*c* site.

TABLE II. Structural parameters for $(Bi_{23.68}Pb_{0.32})(Bi_{1.28}Pb_{0.72})O_{38.48}$.

$Bi_{24}PbO_{37} \equiv (Bi_{23.68}Pb_{0.32})(Bi_{1.28}Pb_{0.72})O_{38.48}$ space group: $I23$, $a = 10.24957(3)$ Å

Atoms	Wyckoff position	x	y	z	B (Å^2)	Bi/Pb occupation
Bi1/Pb1	24*f*	0.8224(1)	0.6795(1)	0.9844(1)	1.07(1)	0.987/0.013
Bi2/Pb2	8*c*	0.011(4)	0.011(4)	0.011(4)	2.6(8)	0.053/0.030
O1	24*f*	0.8607(1)	0.7426(2)	0.496(3)	1.7(3)	1
O2	8*c*	0.8139(2)	0.8139(2)	0.8139(2)	1.7(3)	0.333
O3	8*c*	0.117(3)	0.117(3)	0.117(3)	1.7(3)	0.250
O4	6*b*	0	0.5	0.5	1.7(3)	0.020

$R_B = 3.06\%$, $R_F = 2.63\%$, $R_{wp} = 10.40\%$, $R_p = 7.96\%$, $R_{exp} = 8.43\%$, $\chi^2 = 1.53$.

yielded the equation

$$\mathrm{BVS/OS} = 0.0040(1)x + 0.855(6), \qquad (1)$$

where x represents the Pb^{2+} content at the 8*c* site. According to Eq. (1), if BVS/OS = 1, then $x = 36\%$. Thus, the formula for the most probable structural model is $(Bi_{23.68}Pb_{0.32})(Bi_{1.28}Pb_{0.72})O_{38.48}$, and this composition was further refined by the Rietveld method.

B. Crystal structure of Pb-doped γ-Bi_2O_3 phase

The results of Rietveld refinement for $Bi_{24}PbO_{37}$ or $(Bi_{23.68}Pb_{0.32})(Bi_{1.28}Pb_{0.72})O_{38.48}$ solid solution are given in Table II, and its X-ray powder diffraction profiles are given in Figure 2. The interatomic distances are listed in Table III. About 1.3% of Bi is substituted by Pb at the 24*f* site, and 36% of Bi is substituted by Pb at the 8*c* site. This allows one to conclude that Pb^{2+} is preferentially situated at the 8*c* site. Otherwise the main structural characteristics follow the well-known pattern of doped γ-Bi_2O_3 phases interpreted according to the R-model (Poleti *et al.*, 2007). The polyhedral presentation of the crystal structure of the title compound is shown in Figure 3.

At the 8*c* site (x, x, x), the cations are surrounded by three oxygen atoms (three symmetry equivalents of O3) forming a trigonal pyramidal geometry with $x = 0.011(4)$ [Figure 4(a)]. Such geometry is typical for As^{3+}, Sb^{3+}, and Bi^{3+}, although more common to As^{3+} and Sb^{3+} with a pronounced electron lone pair effect (Makovicky, 1997). The Bi2/Pb2–O bond distances (2.15 vs. 1.95 Å) and Bi2/Pb2 ADP value (2.6 vs. 4.4–5.3 Å^2) are much more reasonable than in the model of Murray *et al.* (1986). It is generally overlooked, but it should be mentioned that around the atoms at the 8*c* site there are three additional O2 atoms at very long distances of 3.24(4) Å forming an irregular 3 + 3 polyhedron around Bi2/Pb2. These three atoms do not contribute significantly to the BVS of Bi2/Pb2 atoms (compare with Bi1/Pb1 atoms), but clearly show the direction of the Bi2/Pb2 lone electron pairs.

Bi1/Pb1 bond distances deviate significantly from the values obtained by Murray *et al.* (1986), but they are in rather good agreement [Table III and Figure 4(b)] with data published for the undoped γ-Bi_2O_3 phase (Radaev *et al.*, 1992). This once again confirms that the Pb content at the 24*f* site is practically negligible. Since the excess positive charge in $(Bi_{23.68}Pb_{0.32})(Bi_{1.28}Pb_{0.72})O_{38.48}$ solid solution is compensated for by partial occupancy of the 6*b* site, if the two farthest O atoms are neglected, one small percentage of Bi1/Pb1 is enclosed by six oxygen ions forming a highly deformed octahedron [Figure 4(c)].

Recently, for a mechanochemically prepared γ-Bi_2O_3 phase with formula $Bi_{2.09}Pb_{1.05}O_{4.17}$ and unit-cell parameter

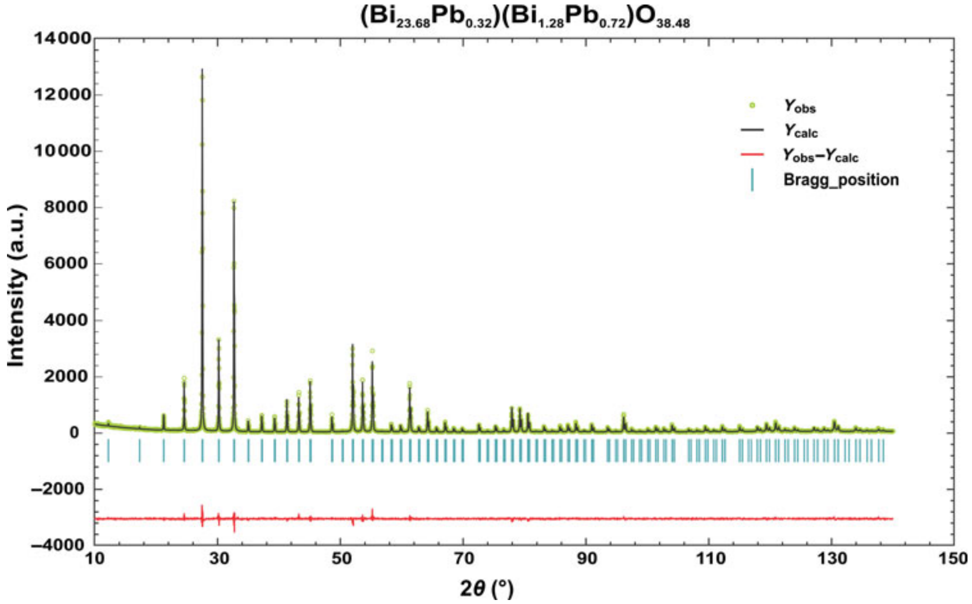

Figure 2. (Color online) Observed, calculated and difference profiles for the Rietveld refinement of $(Bi_{23.68}Pb_{0.32})(Bi_{1.28}Pb_{0.72})O_{38.48}$ compound.

TABLE III. Comparison of interatomic distances for $Bi_{24}PbO_{37}$ (this study), $Bi_{24}Pb_2O_{38}$ (Murray *et al.*, 1986) and $Bi_{12.8}O_{19.2}$ (Radaev *et al.*, 1992) compounds.

	Distance (Å)		
Bond	$Bi_{24}PbO_{37}$	$Bi_{24}Pb_2O_{38}$	$Bi_{12.8}O_{19.2}$
Bi1/Pb1–O1	2.04(2)	2.09	2.045
Bi1/Pb1–O2	2.23(2)	2.22	2.278
Bi1/Pb1–O1	2.41(2)	2.23	2.402
Bi1/Pb1–O1	2.53(2)	2.61	2.456
Bi1/Pb1–O3	2.57(3)	2.63	2.561
Bi1/Pb1–O4	2.593(1)	–	–
Bi1/Pb1–O1	2.96(3)	3.12	3.083
Bi1/Pb1–O1	3.26(3)	3.26	3.287
Bi2/Pb2–O3[a]	2.15(5) × 3	1.94 × 3[b]	1.980 × 3[b]
Bi2/Pb2–O2[b]	3.24(4) × 3	3.38 × 3[b]	3.327 × 3[b]

[a] Only Bi2 in the case of $Bi_{12.8}O_{19.2}$.

[b] Bi2/Pb2 or Bi2 is positioned at the 2*a* site with coordinates 000; O3 vacancies are also present.

a = 10.262(6) Å, a small shift of the *M* cation from the tetrahedral 2*a* to the 8*c* site was also noticed (Zyryanov, 2004). According to this study, all Pb^{2+} is positioned at the 24*f* site and the 8*c* site is only partially occupied by Bi^{3+}, with a Bi2–O3 distance of 2.20(2) Å. Therefore, the structural formula of the investigated sample is $(Bi1_{15.6}Pb1_{8.4})(Bi2_{1.12})O_{33.36}$, and the distribution of cations is just the opposite of our conclusions. However, the credibility of these results is questionable. For example, the ADP of Bi2 is equal to 0 within 3σ, whereas BVS values for cationic sites are 3.37 v.u. for the 8*c* site and 2.26 v.u. for the 24*f* site.

IV. CONCLUSION

The yellow powder of single Pb-doped γ-Bi_2O_3 phase with nominal composition $Bi_{24}PbO_{37}$ was easily prepared starting from a mixture of bismite (α-Bi_2O_3) and massicot (PbO) after heat treatment at 690 °C for 1.5 h. The sample was characterized by the Rietveld method using X-ray powder diffraction data, but it was necessary to apply bond valence calculations to resolve ambiguity about cation distribution over the two mixed sites. This approach yielded $(Bi_{23.68}Pb_{0.32})(Bi_{1.28}Pb_{0.72})O_{38.48}$ as the most probable structural formula. According to this formula, Pb^{2+} is preferentially situated at the 8*c* site, i.e. only 1.3% of Bi^{3+} is substituted by Pb^{2+} at the 24*f* site and 36% of occupied sites at the 8*c* site.

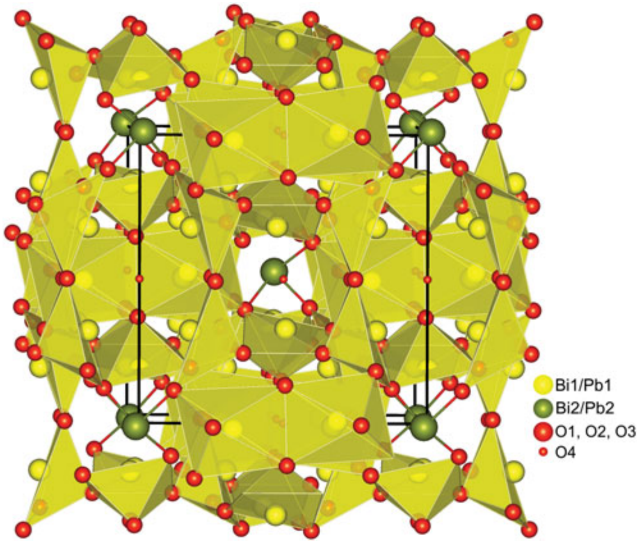

Figure 3. (Color online) Polyhedral presentation of $(Bi_{23.68}Pb_{0.32})(Bi_{1.28}Pb_{0.72})O_{38.48}$ compound.

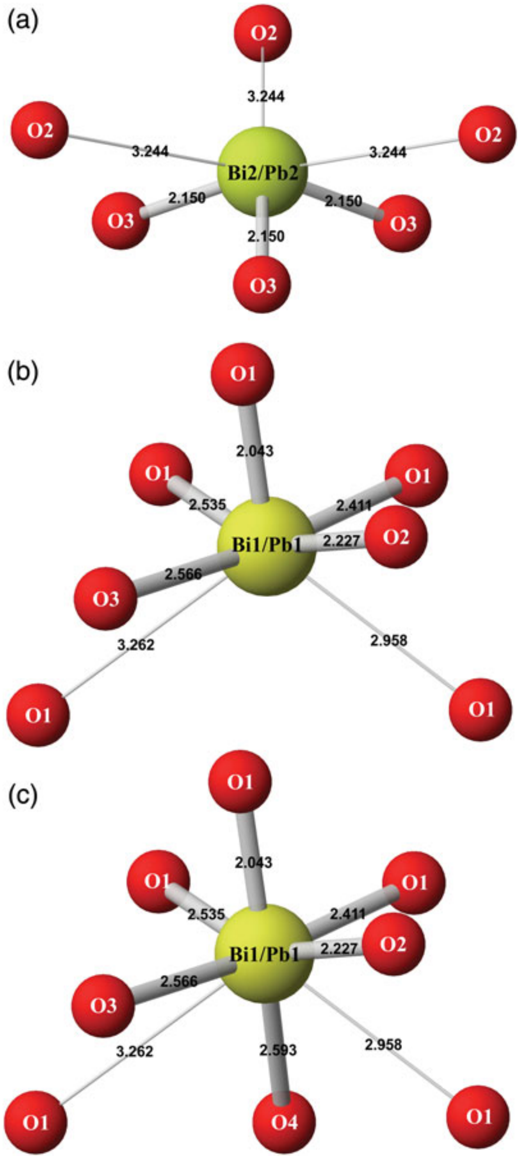

Figure 4. (Color online) Geometry of 8*c* (a) and 24*f* sites (b, c).

Apart from the typical properties of sillenite structure, the investigated structure of Pb-doped γ-Bi_2O_3 phase, $Bi_{24}PbO_{37}$, possesses some exceptional characteristics: novel chemical composition and the occurrence of two crystallographic independent mixed cationic sites, one of which is slightly [$x = 0.011(4)$ Å] moved from the origin and center of the unit cell (2*a* site) along the [111]-direction. The key to the exceptional properties of Pb-doped γ-Bi_2O_3 phase lies in the fact that both Pb^{2+} and Bi^{3+} are large, isoelectronic ions of similar sizes, with the lone electron pair. Therefore, the relatively small tetrahedral 2*a* site is not suitable for them, and as a result the transformation of the fully occupied 2*a* site to the partly occupied 8*c* site appears. At the partly occupied 8*c* site, Bi2/Pb2 cations with three O^{2-} ions form a trigonal pyramid with cations at the apex of the pyramid.

ACKNOWLEDGMENTS

The authors gratefully acknowledge financial support from the Ministry of Education and Science of the Republic of Serbia (Grant No. III 45007).

Borowiec, M. T., Kozankiewicz, B., Szymczak, H., Zmija, J., Majchrowski, A., Zaleski, M., and Zayarnyuk, T. (**1999**). "Photoconductivity of $Bi_{12}Ti_{1-x}Pb_xO_{20}$ single crystal," Acta Phys. Pol. A **96**, 785–792.

Brese, N. E. and O'Keeffe, M. (**1991**). "Bond valence parameters for solids," J. Am. Chem. Soc. **113**, 3226–3229.

Brown, I. D. (**2009**). *The Chemical Bond in Inorganic Chemistry: The Bond Valence Model* (Oxford University Press, Oxford) p. 26–40.

Brown, I. D. and Altermatt, D. (**1985**). "Bond–valence parameters obtained from a systematic analysis of the Inorganic Crystal Structure Database," Acta Crystallogr. Sect. B: Struct. Sci. **41**, 244–247.

Cornei, N., Tancret, N., Abraham, F., and Mentre, O. (**2006**). "New ε-Bi_2O_3 metastable polymorph," Inorg. Chem. **45**, 4886–4888.

Craig, D. C. and Stephenson, N. C. (**1975**). "Structural studies of some body centered cubic phases of mixed oxides involving Bi_2O_3: the structures of $Bi_{25}FeO_{40}$ and $Bi_{38}ZnO_{60}$," J. Solid State Chem. **15**, 1–8.

Darriet, J., Launaya, J. C., and Zuniga, F. J. (**2005**). "Crystal structures of the ionic conductors $Bi_{46}M_8O_{89}$ (M = P, V) related to the fluorite-type structure," J. Solid State Chem. **178**, 1753–1764.

Fee, M. G. and Long, N. J. (**1996**). "Mixed conductivity in metal-doped bismuth-lead oxide," Solid State Ionics **86–88**, 733–737.

Fee, M. G., Sammes, N. M., Tomsett, G., Soto, T., and Cartner, A. M. (**1997**). "The effect of heat treatment on the physical and electrical properties of the fast ion conductor $Bi_8Pb_5O_{17}$," Solid State Ionics **95**, 183–189.

Gattow, G. and Schröder, H. (**1962**). "Über wismutoxide. III. Die kristallstruktur der hochtemperaturmodifikation von wismut(III)-oxid (δ-Bi_2O_3)," Z. Anorg. Allg. Chem. **318**, 176–189.

Ghedia, S., Locherer, T., Dinnebier, R., Prasad, D. L. V. K., Wedig, U., Jansen, M., and Senyshyn, A. (**2010**). "High-pressure and high-temperature multianvil synthesis of metastable polymorphs of Bi_2O_3: crystal structure and electronic properties," Phys. Rev. B **82**, 1–12.

Gualtieri, A. F., Imovilli, S., and Prudenziati, M. (**1997**). "Powder X-ray diffraction data for the new polymorphic compound ω-Bi_2O_3," Powder Diffr. **12**, 90–92.

Harwig, H. A. (**1978**). "On the structure of bismuthsesquioxide: the α-, β-, γ- and δ-phase," Z. Anorg. Allg. Chem. **444**, 151–166.

Harwig, H. A. and Gerards, A. G. (**1979**). "The polymorphism of bismuth sesquioxide," Thermochim. Acta **28**, 121–131.

Harwig, H. A. and Weenk, J. W. (**1978**). "Phase relationships in bismuth sesquioxide," Z. Anorg. Allg. Chem. **444**, 167–177.

Hill, R. J. (**1992**). "International union of crystallography. Commission on powder diffraction. Rietveld refinement round robin. I. Analysis of standard X-ray and neutron data for $PbSO_4$," J. Appl. Crystallogr. **25**, 589–610.

Hill, R. J. and Cranswick, L. M. D. (**1994**). "International union of crystallography. Commission on powder diffraction. Rietveld refinement round Robin. II. Analysis of monoclinic ZrO_2," J. Appl. Crystallogr. **25**, 589–610.

Honnart, F., Boivin, J. C., Thomas, D., and De Vries, K. J. (**1983**). "Bismuth-lead oxide, a new highly conductive oxygen materials," Solid State Ionics **9–10**, 921–924.

Karanović, Lj., Petrović-Prelević, I., and Poleti, D. (**1999**). "A practical approach to Rietveld analysis. Comparison of some programs running on personal computers," Powder Diffr. **14**, 171–170.

Knoblochova, K., Ticha, H., Schwarz, J., and Tichy, L. (**2009**). "Raman spectra and optical properties of selected Bi_2O_3–PbO–B_2O_3–GeO_2 glasses," Opt. Mater. **31**, 895–898.

Levin, E. M. and Roth, R. S. (**1964a**). "Polymorphism of bismuth sesquioxide. I. Pure Bi_2O_3," J. Res. Nat. Bur. Stand., Sect. A. Phys. Chem. **68**(2), 189–195.

Levin, E. M. and Roth, R. S. (**1964b**). "Polymorphism of bismuth sesquioxide. II. Effect of oxide additions on the polymorphism of Bi_2O_3," J. Res. Nat. Bur. Stand., Sect. A. Phys. Chem. **68**, 197–206.

Makovicky, E. (**1997**). "Modular crystal chemistry of sulphosalts and other complex sulfides," in *Modular Aspects of Minerals, EMU Notes Mineral*, edited by S. Merlino (Eötvös University Press, Budapest), Vol. **1**, p. 237–271.

Manier, M., Champarnaud-Mesjard, J. C., Mercurio, J. P., Bernache, D., and Frit, B. (**1988**). "Synthesis, sintering and dielectric properties of a new bismuth–lead–antimony oxide $Bi_3Pb_4Sb_5O_{21}$," Mater. Chem. Phys. **19**, 167–178.

Mazumdar, S. (**1993**). "Structure determination of $PbBi_{12}O_{20}$ from X-ray powder diffraction," Indian J. Phys. **67**(A), 45–52.

McCusker, L. B., Von Dreele, R. B., Cox, D. E., Louër, D., and Scardi, P. (**1999**). "Rietveld refinement guidelines," J. Appl. Cryst. **32**, 36–50.

Mitsuyu, T., Wasa, K., and Hayakawa, S. (**1976**). "Piezoelectric thin films of RF-sputtered $Bi_{12}PbO_{19}$," J. Appl. Phys. **47**, 2901–2902.

Murray, A. D., Catlow, C. R. A., Beech, F., and Drennan, J (**1986**). "A neutron powder diffraction study of the low- and high-temperature structures of $Bi_{12}PbO_{19}$," J. Solid State Chem. **62**, 290–296.

Pan, A. and Ghosh, A. (**2000**). "A new family of lead–bismuthate glass with a large transmitting window," J. Non-Cryst. Solids. **271**, 157–161.

Pang, G., Feng, S., Tang, Y., and Xu, R. (**1998**). "Hydrothermal synthesis, characterization, and ionic conductivity of vanadium-stabilized $Bi_{17}V_3O_{33}$ with fluorite-related superlattice structure," Chem. Mater. **10**, 2446–2449.

Poleti, D., Karanović, Lj., and Hadži-Tonić, A. (**2007**). "Doped γ-Bi_2O_3: synthesis of microcrystalline samples and crystal chemical analysis of structural data," Z. Kristallogr. **222**, 59–72.

Radaev, S. F., Muradyan, L. A., and Simonov, V. I. (**1991**). "Atomic structure and crystal chemistry of sillenites: $Bi_{12}(Bi^{3+}_{0.50}Fe^{3+}_{0.50})O_{19.50}$ and $Bi_{12}(Bi^{3+}_{0.67}Zn^{2+}_{0.33})O_{19.33}$," Acta Crystallogr., Sect. B: Struct. Sci. **47**, 1–6.

Radaev, S. F. and Simonov, V. I. (**1992**). "Struktura sillenitov i atomnye mehanizmy izomorfnyh zameshchanii v nih," Kristallografiya **37**, 914–941.

Radaev, S. F., Simonov, V. I., and Kargin, Yu. F. (**1992**). "Structural features of γ-Phase Bi_2O_3 and its place in the sillenite family," Acta Crystallogr., Sect. B: Struct. Sci. **48**, 604–609.

Rangavittal, N., Row, T. N. G., and Rao, C. N. R. (**1994**). "A study of cubic bismuth oxides of the type $Bi_{26-x}M_xO_{40-d}$ (M = Ti, Mn, Fe, Co, Ni or Pb) related to γ-Bi_2O_3," Eur. J. Solid State Inorg. Chem. **31**, 409–422.

Reshak, A. H., Lakshminarayana, G., Proskurina, G., Yushanin, V. G., Calus, S., Chmiel, M., Miedzinski, R., and Brik, M. G. (**2010**). "Laser induced effects in PbO–Bi_2O_3–Ga_2O_3–BaO: Eu glasses," Opt. Commun. **283**, 3049–3051.

Rodriguez-Carvajal, J. (**1993**). "Recent advances in magnetic structure determination by neutron powder diffraction," Physica B **192**, 55–69.

Roisnel, T. and Rodriguez-Carvajal, J. (**2001**). "WinPLOTR: a windows tool for powder diffraction pattern analysis," Mater. Sci. Forum **378–381**, 118–123.

Salem, S. M. and Mohamed, E. A. (**2011**). "Electrical conductivity and dielectric properties of Bi_2O_3–GeO_2–PbO–MoO_3 glasses," J. Non-Cryst. Solids **357**, 1153–1159.

Sammes, N. M., Tompsett, G., and Cartner, A. M. (**1995**). "Characterization of bismuth lead oxide by vibrational spectroscopy," J. Mater. Sci. **30**, 4299–4308.

Sammes, N. M., Tompsett, G. A., Näfe, H., and Aldinger, F. (**1999**). "Bismuth based oxide electrolytes-structure and ionic conductivity," J. Eur. Ceram. Soc. **19**, 1801–1826.

Shi, D. M. and Qian, Q. (**2010**). "Spectroscopic properties and energy transfer in Ga_2O_3-Bi_2O_3-PbO-GeO_2 glasses doped with Er^{3+} and Tm^{3+}," Physica B **405**, 2503–2507.

Shuk, P., Wiemhofer, H.-D., Guth, U., Gijpel, W., and Greenblatt, M. (**1996**). "Oxide ion conducting solid electrolytes based on Bi_2O_3," Solid State Ionics **89**, 179–196.

Sillén, L. G. (**1937**). "X-ray studies on bismuth trioxide," Ark. Kemi. Miner. Geol. **12A**, 1–15.

Valant, M. and Suvorov, D. (**2001**). "Processing and dielectric properties of sillenite compounds $Bi_{12}MO_{20-\delta}$ (M = Si, Ge, Ti, Pb, Mn, $B_{1/2}P_{1/2}$)," J. Am. Ceram. Soc. **84**, 2900–2904.

Valant, M. and Suvorov, D. (**2002**). "A stoichiometric model for sillenites," Chem. Mater. **14**, 3471–3476.

Watanabe, A. (**1997**). "$Bi_{23}M_4O_{44.5}$ (M = P and V): New oxide-ion conductors with triclinic structure based on a pseudo-fcc subcell," Solid State Ionics **96**, 75–81.

Young, R. A. and Wiles, D. B. (**1982**). "Profile shape functions in Rietveld refinements," J. Appl. Crystallogr. **15**, 430–438.

Zyryanov, V. V. (**2004**). "Structure and thermal behavior of metastable sillenites prepared by mechanochemical synthesis," J. Struct. Chem. **45**, 454–464.